
Advanced Composite Materials
Publication details, including instructions for authors and subscription information:
http://www.tandfonline.com/loi/tacm20

# Experimental study on impact tensile property of glass fiber

Norihiko Taniguchi [a], Yoshihiko Arao [b], Tsuyoshi Nishiwaki [a], Norio Hirayama [c], Koichi Nakamura [c] & Hiroyuki Kawada [d]

[a] Institute of Sports Science, ASICS Corporation, Kobe, Japan

[b] Department of Mechanical and Systems Engineering, Doshisha University, Kyoto, Japan

[c] Research and Development Head Office, Nitto Boseki Co., Ltd, Japan

[d] Department of Applied Mechanics and Aerospace Engineering, Waseda University, Tokyo, Japan

Version of record first published: 06 Aug 2012.

To cite this article: Norihiko Taniguchi , Yoshihiko Arao , Tsuyoshi Nishiwaki , Norio Hirayama , Koichi Nakamura & Hiroyuki Kawada (2012): Experimental study on impact tensile property of glass fiber, Advanced Composite Materials, 21:2, 165-175

To link to this article: http://dx.doi.org/10.1080/09243046.2012.688496

*Advanced Composite Materials*
Vol. 21, No. 2, April 2012, 165–175



# Experimental study on impact tensile property of glass fiber

Norihiko Taniguchi[a]*, Yoshihiko Arao[b], Tsuyoshi Nishiwaki[a], Norio Hirayama[c], Koichi Nakamura[c] and Hiroyuki Kawada[d]

[a]*Institute of Sports Science, ASICS Corporation, Kobe, Japan;* [b]*Department of Mechanical and Systems Engineering, Doshisha University, Kyoto, Japan;* [c]*Research and Development Head Office, Nitto Boseki Co., Ltd, Japan;* [d]*Department of Applied Mechanics and Aerospace Engineering, Waseda University, Tokyo, Japan*

(*Received 28 February 2012; accepted 3 April 2012*)

The tensile properties of E-glass, which is the most popular reinforcement fiber in composite materials, were determined from the experimental results of fiber bundle testing under a high strain rate. The tests were performed by using two types of experimental methods. One is the tension-type split Hopkinson bar system and the other is the universal high-speed tensile-testing machine. In the results, it was demonstrated that the tensile strength and fracture strain of E-glass fiber increased with the strain rate. The absorbed strain energy, therefore, significantly increased. It was also shown that the strain rate dependency of E-glass fiber tensile strength was strongly affected by fiber diameter. The smaller diameter of E-glass fiber has the stronger strain rate dependency. Finally, the impact tensile strengths of high-strength glass and carbon fibers were investigated. It was confirmed that the tensile strength of the high-strength glass fiber also increased with the strain rate, but the tensile properties of carbon fiber were almost independent of the strain rate.

**Keywords:** glass fiber; impact property; strain rate effect; tensile strength; energy absorption



## 1. Introduction

The use of composite materials in the fields of sport and automotive has been growing since these materials exhibit high stiffness, strength, and low density [1]. To design composite structure in the above fields, the impact properties such as the energy absorption property and strength are very important. Therefore, characterizing the impact properties of composite materials can be essential. According to the previous studies[2–5], the composite material as represented by fiber-reinforced plastics (FRP) shows the strain rate dependency on mechanical property. The authors investigated the strain rate effect on tensile properties of unidirectional FRP based on thermoplastic epoxy resin [6]. They demonstrated that the tensile strength was almost independent of the strain rate in case that carbon fiber was employed as reinforcement. On the other hand, those of E-glass and high-strength glass fiber composites were obviously affected by the strain rate. Staab and Gilat [7] investigated the effects of tensile strength in the case of angle-ply glass/epoxy laminates. They concluded that the fibers had a greater influence on the strain rate effect than the matrix. These may be useful information to design the composite structure in the above industrial fields. However, the impact properties of glass fiber itself must be investigated for the application.

*Corresponding author. Email: taniguchi-no@asics.co.jp

ISSN 0924-3046 print/ISSN 1568-5519 online

http://dx.doi.org/10.1080/09243046.2012.688496
http://www.tandfonline.com

Limited data on impact property of glass fiber have been obtained by Xia et al. [8,9]. They proposed the statistical model from the impact tensile test of E-glass fiber bundle. Their model prediction was in good agreement with the experimental data. However, the further discussion, such as the effect of glass fiber diameter and material constitution, must be needed.

This study aims to characterize the impact tensile properties of glass fiber. In order to discuss the effect of strain rate on the properties, typical E-glass bundle is tested at the static and impact loading conditions. Furthermore, the effect of fiber diameter on the strain rate dependency of tensile strength is investigated. Finally, the energy absorption property of E-glass fiber is compared with those of high-strength glass and typical carbon fibers.

## 2. Experiment

E-glass bundle specimen was employed as shown in Figure 1. The average diameter of single filament is 17.0 μm and the number of fiber is 1000. The aluminum tabs are glued at both the ends of the specimen. In this study, the impact tensile properties were measured from two types of experimental machines. One is the tension-type split Hopkinson bar (SHB) apparatus. And the other is the high-speed tensile testing machine controlled by hydraulic pressure (Hydroshot HITS-T10, Shimadzu Corporation). Figure 2 shows a schematic drawing of tension-type SHB apparatus in this study [6]. It consists of an input bar with a flange, an output bar, and a cylindrical striker. The data obtained from the SHB method comprise the strain histories of the input and output bars. In this study, the strain histories are recorded from the strain gages with a gage length of 1.0 mm at a sampling rate of 1.0 MHz via a DC amplifier (upper frequency limit: 100 kHz). In the SHB system, the stress, strain, and strain rate can be calculated by the one-dimensional wave propagation theory [10], that is,

$$\sigma = \frac{AE\varepsilon_t}{NA_s}, \tag{1}$$

$$\varepsilon = -\frac{2c_0}{l_0}\int_0^t \varepsilon_r d\tau, \tag{2}$$

$$\dot{\varepsilon} = -\frac{2c_0}{l_0}\varepsilon_r, \tag{3}$$

where $\varepsilon_r$ and $\varepsilon_t$ denote the reflected and transmitted strain waves, respectively. Further, $E$ denotes the bar's Young's modulus; $A$, the bar's cross-sectional area; $A_s$, the fiber's

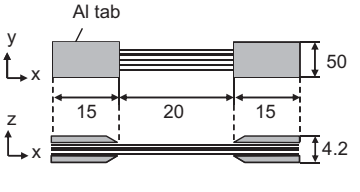


Figure 1. Geometry of specimen used in this study.

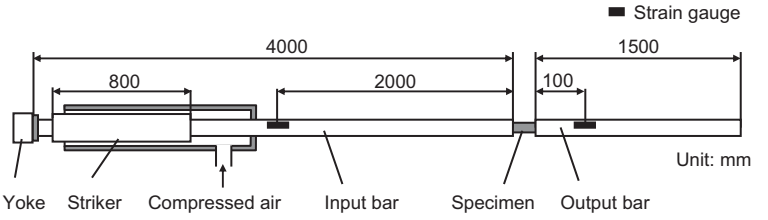


Figure 2. Tension-type SHB apparatus used in this study.

cross-sectional area; $N$, the number of fiber; $c_0$, the elastic wave speed; and $l_0$, the specimen's gage length.

Compared with the SHB apparatus used in this study, the testing speed and displacement of the high-speed tensile testing machine is very large. Namely, it is possible to carry out the impact tensile test in higher range of strain rate. However, it is suggested from the specification that the prospective maximum displacement, which is approximately 1.0 mm in this study, may be beyond the error tolerance level of the testing machine. Therefore, only stress history of the specimen was measured at a sampling rate of 1.0 MHz.

## 3. Experimental result

### *3.1. Stress–strain curve*

Typical example of stress–strain curve for E-glass fiber, whose average strain rate is $250\,s^{-1}$, is shown in Figure 3. Stress–strain curve under quasi-static loading condition, the average strain rate of $8.33 \times 10^{-4}\,s^{-1}$, is also shown in Figure 3 for comparison. It is shown that the initial slope of stress–strain relationship between quasi-static and strain rate of $250\,s^{-1}$ is almost same. However, the maximum stress and strain at the strain rate of $250\,s^{-1}$ are much larger than those at quasi-static condition.

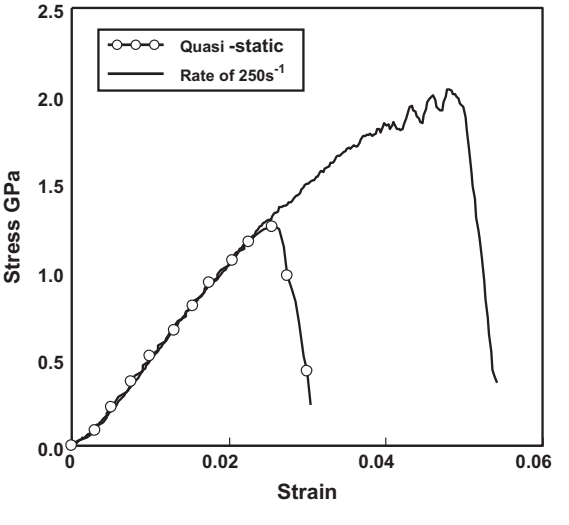


Figure 3. Comparison of stress–strain curves between quasi-static and strain rate of $250\,s^{-1}$ from E-glass bundle test.

### 3.2. Dependence of strain rate on mechanical property

The relationships between strain rate and representative mechanical properties are shown in Figure 4(a)–(c). In this study, the maximum stress and strain in Figure 3 are defined as tensile strength and fracture strain As already presented, the data obtained from the high-speed tensile testing machine is just a stress history. Thus, the strain rate effect on Young's modulus and fracture strain was investigated from the experimental data of the tension-type SHB apparatus only. In Figure 4(a), it is demonstrated that the resultant Young's modulus is almost independent of strain rate. This phenomenon is caused by that E-glass fiber behaves almost elastically. The tensile strength of E-glass fiber is plotted in Figure 4(b) as a function of strain rate. In this figure, it is implied that the tensile strength increases with the strain rate. Furthermore, it significantly increases in the strain rate range from $8.33 \times 10^{-4}$ to $50\,s^{-1}$. Beyond the strain rate of $50\,s^{-1}$, it tends to increase slightly. Its increasing ratio from quasi-static condition to the strain rate of $250\,s^{-1}$ is almost 60%. This tendency is the same as that of Xia's work [9]. It can be concluded that the strain rate effect of tensile strength for unidirectional GFRP reported in Ref. [6] is mainly due to that for glass fiber.

Although there are some reasons about the strain rate dependency of tensile strength for glass fiber: (1) temperature rise during the test, (2) effect of thermal residual stress, and (3) molecular structure, we have an eye on a subcritical crack growth which is unique characteristic of glass. According to classical linear elastic fracture mechanics, an apparent glass fiber strength $\sigma_f$ can be described as follows.

$$\sigma_f = \frac{K_c}{Y(a) \cdot \sqrt{\pi a(t)}}, \tag{4}$$

where $K_c$ is critical stress intensity factor, and $Y(a)$ and $a(t)$ are the geometric correction factor and crack length, respectively.

Suratwala [11] and Freiman [12] reported the presence of subcritical crack growth region before final fracture of glass. Since crack length is a function of time as shown in Equation (4), it may be possible that the length of subcritical crack growth at final fracture under

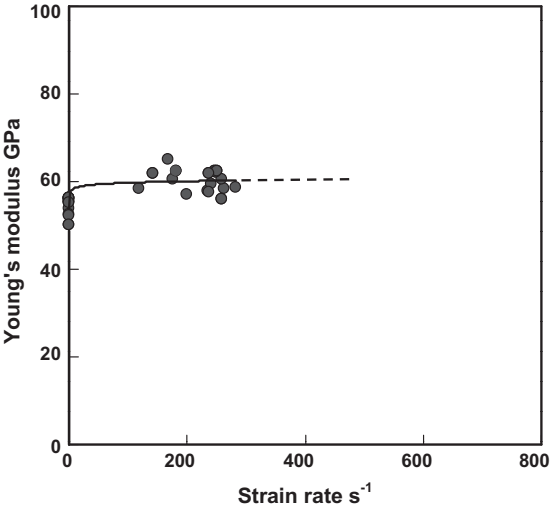


Figure 4(a). Dependence of strain rate on Young's modulus of E-glass fiber.

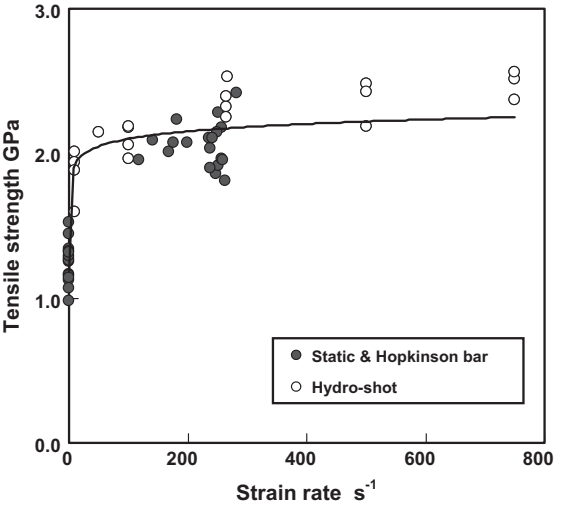


Figure 4(b). Dependence of strain rate on tensile strength of E-glass fiber.

quasi-static loading condition is different from that under impact loading condition. As a result, tensile strength of glass fiber increases with strain rate. However, there is room for further investigation. The experimental or theoretical verifications are the challenges for the future.

The fracture strain of E-glass fiber is plotted in Figure 4(c) as a function of strain rate. Although the experimental data are obviously scattered, the fracture strain increases with the strain rate.

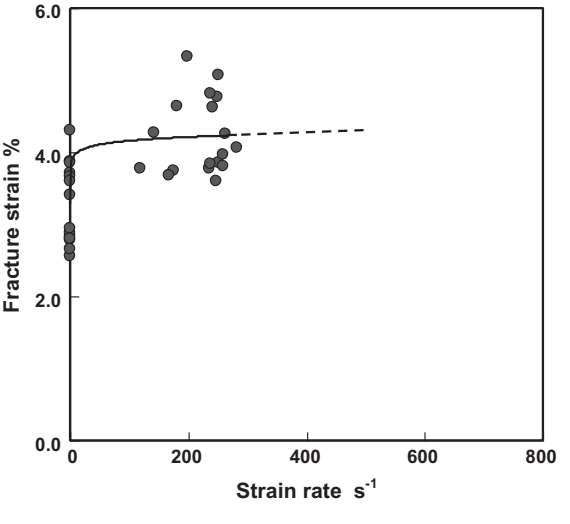


Figure 4(c). Dependence of strain rate on fracture strain of E-glass fiber.

### 3.3. *Fracture behavior of E-glass fiber*

In order to investigate the strain rate effect on the mechanical properties of E-glass fiber more precisely, fracture behavior was recorded using a digital high-speed video camera (HyperVision HPV-2, Shimadzu Corporation). Figure 5 shows the summary of photographs at the strain rate of $8.33 \times 10^{-4}$, 10, 100, 250, and $500\,s^{-1}$ when the applied stress reached at just after the maximum value. It is clear that E-glass fiber was reduced to shorter particles with increasing of strain rate. The further experiment was conducted about the above results. Fracture behavior of three E-glass fibers, whose diameter is 100 μm, was recorded under tensile loading at the strain rate of $500\,s^{-1}$. A series of fracture progressive photographs are shown in Figure 6(a–e). First of all, fiber break occurs at the single point as shown in Figure 6(b, c). And then, it is confirmed that each fiber is getting shattered in Figure 6(d, e). This phenomenon is caused by the stress wave propagation effect within E-glass fiber after breakage. Judging from these results, it is concluded that the shattered fracture behavior of E-glass fiber bundle in Figure 5 is due to the stress wave propagation effect after fiber breakage. Thus, the fracture behavior change from quasi-static to high strain rate condition has little effect on the strain rate dependency of tensile strength for E-glass fiber.

## 4. Discussion

### 4.1. *Effect of fiber diameter on strain rate dependency*

Generally, the tensile strength of glass fiber is determined by pre-existing surface flaws, which occur with a statistical nature. This increases the probability of encountering a more severe flaw with increase in surface area. Thus, it is important for material designing to understand the effect of E-glass fiber diameter on strain rate dependency of tensile strength. In this section, five types of E-glass fiber bundles whose average diameters are 3.2, 5.3, 7.2, 9.2, and 13.8 μm were tested and compared. The specification of specimen is summarized in Table 1. The important point to note is that the average fiber diameter is controlled by changing the spinning speed of E-glass fiber in this study. The tensile strength for each fiber diameters is plotted in Figure 7 as a function of strain rate with the data from Figure 4(b). In this figure, the experimental result of E-glass plate is also demonstrated as a reference. The E-glass plate specimen has the gage length of 20 mm, the width of 5.0 mm, and the thickness of 0.5 mm. The surfaces of specimen are mirror polished. As well as the case of E-glass bundle specimen, the aluminum tabs are glued at the ends. As clearly shown in Figure 7, any types of specimens show strain rate dependency. The tensile strength increases with strain rate. However, it is confirmed that the tensile strength of E-glass plate is relatively less affected by strain rate as compared with that of bundle specimens.

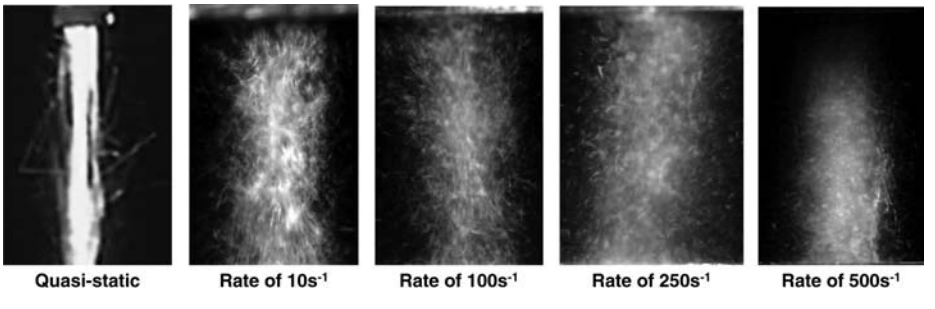


Figure 5. Comparisons of fracture behavior in E-glass bundle.

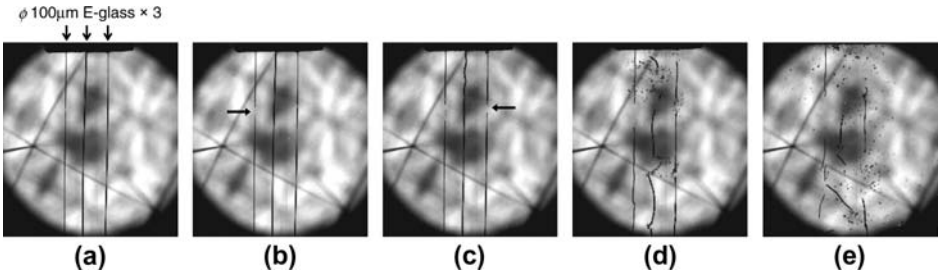


Figure 6. Successive photographs of fracture in f100 mm E-glass specimen at the rate of 500 $s^{-1}$.

Table 1. Specification of E-glass bundle specimens used in this study.

| Specimen | EG 17 | EG 13.8 | EG 9.2 | EG 7.5 | EG 5.3 | EG 3.2 |
|---|---|---|---|---|---|---|
| Average diameter (μm) | 17.0 | 13.8 | 9.2 | 7.5 | 5.3 | 3.2 |
| Number of fiber | 1000 | 906 | 200 | 200 | 200 | 1600 |

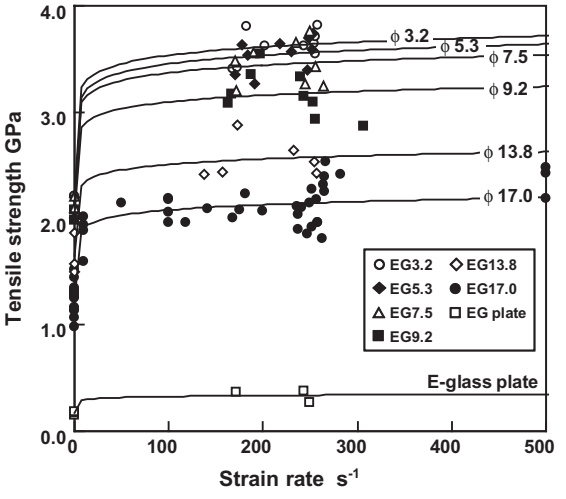


Figure 7. Dependence of strain rate on tensile strength of E-glass fibers and plate.

Figure 8 shows the relationship between tensile strength and fiber diameter at static and strain rate of 250 $s^{-1}$. It is confirmed that the tensile strength at the strain rate of 250 $s^{-1}$ is higher than those at static loading condition for any fiber diameter. The average increments of tensile strength from static to strain rate of 250 $s^{-1}$ are 1.46 GPa (diameter of $\phi = 3.2$ μm), 1.49 GPa ($\phi = 5.3$ μm), 1.31 GPa ($\phi = 7.2$ μm), 1.09 GPa ($\phi = 9.2$ μm), 0.89 GPa ($\phi = 13.8$ μm), and 0.87 GPa ($\phi = 17.0$ μm), respectively. The smaller diameter of E-glass fiber causes the higher tensile strength and strength increment at both strain rate conditions. Judging from these results, it is concluded that the fiber diameter makes a great influence on the strain rate dependency of tensile strength. Furthermore, these results also imply that the characteristic of E-glass fiber surface is one of the important factors for characterizing the strain rate dependency.

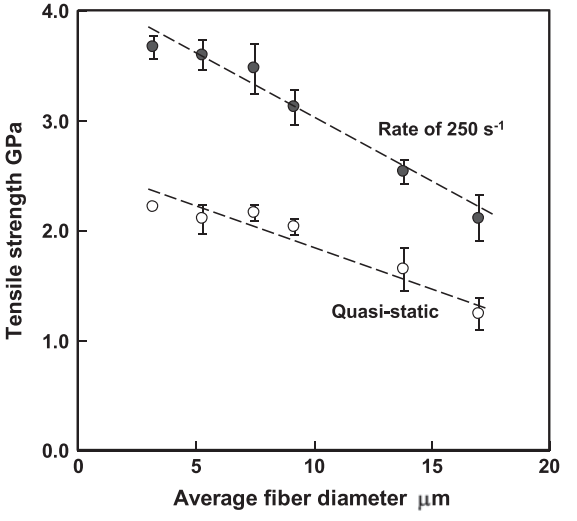


Figure 8. Comparison of tensile strength between quasi-static and strain rate of 250 $s^{-1}$ for representative fiber diameters.

### 4.2. *Effect of reinforcement fiber type on strain rate dependency*

The experimental data of the strain rate dependency for various reinforcement fibers are useful not only for unified discussion but also the practical designing of composite materials. In this section, high-strength glass (T-glass, Nitto Boseki Co., Ltd) and typical carbon fiber (Torayca T300, Toray Industries, Inc.) bundles were tested. The specification of specimen used in this section is summarized in Table 2. The resultant stress–strain curves under static and strain rate of 250 $s^{-1}$ are shown in Figure 9(a) and (b), respectively. As well as E-glass fiber, the resultant Young's modulus of both fibers is almost independent of strain rate. The tensile strengths are plotted in Figure 10 as a function of strain rate. It is confirmed that the tensile strength of high-strength glass increase with the strain rate. These results cause better energy absorption property under impact loading condition rather than those of carbon fibers. Figure 11 shows the relationship between the absorbed specific strain energy at maximum tensile stress and strain rate. It is confirmed that the experimental data of glass fibers significantly increase with strain rate, while that of carbon fiber is almost constant. The mean values under static loading condition are 8.54 J/g for E-glass fiber, 19.8 J/g for high-strength glass fiber, and 10.7 J/g for carbon fiber. On the other hand, those at strain rate of 250 $s^{-1}$ are 17.9 J/g for E-glass fiber, 32.2 J/g for high-strength glass fiber, and 11.6 J/g for carbon fiber. It is shown that those of glass fiber at strain rate of 250 $s^{-1}$ are 1.5–2.8 times higher than those of carbon fibers. Judging from these results, it is concluded that the glass fibers possess higher energy absorption properties under impact loading conditions rather than carbon fibers.

Table 2. Specification of E-glass bundle specimens used in this study.

| | E-glass | High-strength glass (T-glass) | Carbon (Torayca T300) |
|---|---|---|---|
| Density (g/$cm^3$) | 2.58 | 2.49 | 1.76 |
| Average diameter (μm) | 17.0 | 13.0 | 6.0 |
| Number of fiber | 1000 | 400 | 1000 |

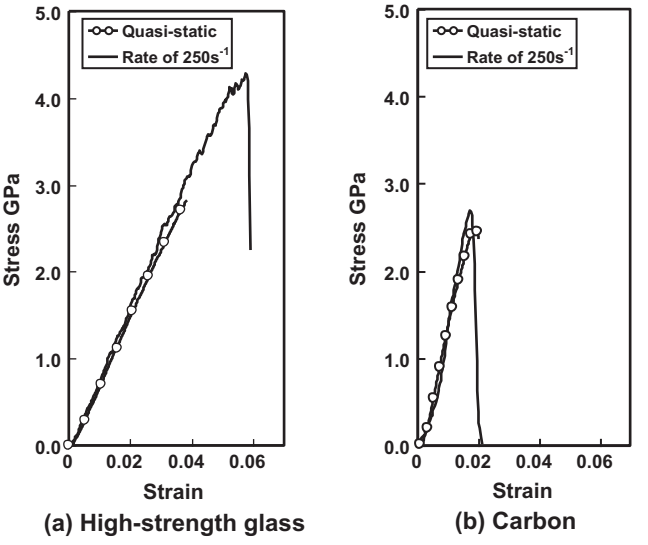


Figure 9. Comparison of stress–strain curves between quasi-static and strain rate of 250 $s^{-1}$ from (a) high-strength glass and (b) carbon fiber bundle test.

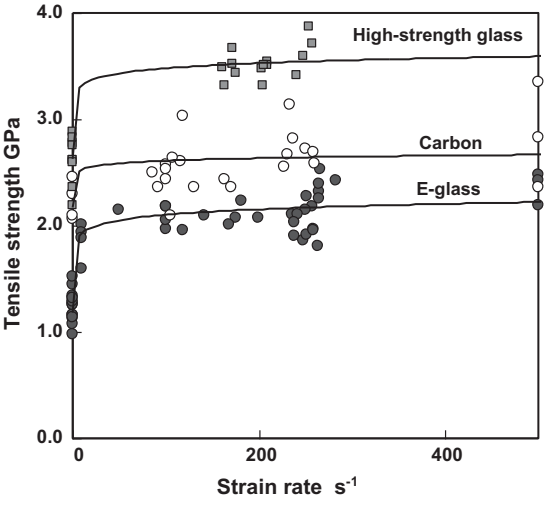


Figure 10. Dependence of strain rate on tensile strength of E-glass, high-strength glass, and carbon fibers.

## 5. Concluding remarks

The tensile properties of E-glass fiber under a high strain rate were experimentally investigated from fiber bundle test. The experimental results showed that the tensile strength and fracture strain of E-glass fiber increased with the strain rate. The effect of fiber diameter on impact tensile strength was discussed. It was shown that the strain rate dependency of E-glass fiber strength was strongly affected by the fiber diameter. In other words, the smaller diameter of E-glass fiber causes the stronger strain rate dependency. The impact tensile properties of

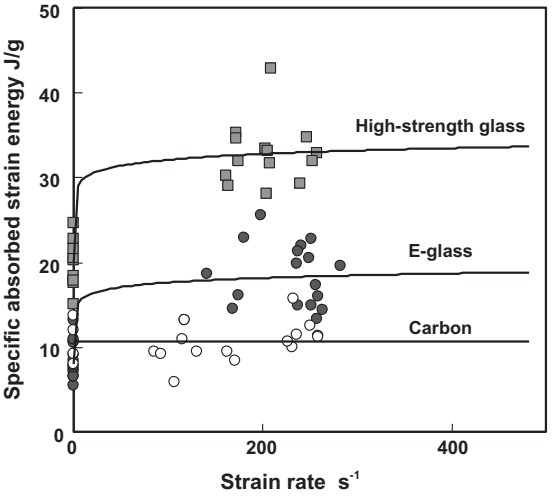


Figure 11. Dependence of strain rate on specific absorbed strain energy of E-glass, high-strength glass, and carbon fibers.

high-strength glass and carbon fibers were also investigated. It was confirmed that the tensile strength of the high-strength glass fiber also increased with the strain rate. On the other hand, the tensile properties of carbon fiber were almost independent of the strain rate. Judging from these results, it is concluded that the glass fibers possess higher energy absorption properties under impact loading conditions rather than carbon fibers.

## Acknowledgement

The authors thank Mr. Hiroya Mita, Shimadzu corporation, for the technical support about the high-speed tensile testing machine.

## References

[1] Nomaguchi K. Journal of the Japan Society for Composite Materials. 2006;32(3):100–12.
[2] Harding J, Welsh LM. A tensile testing technique for fibre-reinforced composites at impact rates of strain. Journal of Materials Science. 1983;18:1810–26.
[3] Harding J. Effect of strain rate and specimen geometry on the compressive strength of woven glass-reinforced epoxy laminates. Composites. 1993;24(4):323–32.
[4] Higashida F, Ogawa K. Impact three-point bending tests on FRP by Split-Hopkinson Bar technique. Journal of The Society of Materials Science, Japan. 1990;39(445):1462–8.
[5] Shokrieh MM, Omidi MJ. Tension behavior of unidirectional glass/epoxy composites under different strain rates. Composite Structures. 2009;88:595–601.
[6] Taniguchi N, Nishiwaki T, Hirayama N, Nishida H, Kawada H. Evaluating the impact tensile properties of unidirectional fibre-reinforced composites with thermoplastic epoxy resin. Transactions of the Japan Society of Mechanical Engineers, Part A. 2009;75(758):1284–9.
[7] Staab GH, Gilat A. High strain rate response of angle-ply glass/epoxy laminates. Journal of Composite Materials. 1995;29(10):1308–20.
[8] Xia Y, Yuan J, Yang B. A statistical model and experimental study of the strain-rate dependence of the strength of fibres. Composites Science and Technology. 1994;52:499–504.
[9] Wang Z, Xia Y. Experimental evaluation of the strength distribution of fibers under high strain rates by bimodal weibull distribution. Composites Science and Technology. 1998;57:1599–607.
[10] Graff KF. Wave motion in elastic solids. Dover publications. ISBN 0-486-66745-6.

[11] Suratwala TI, Steele RA. Anomalous temperature dependence of sub-critical crack growth in silica glass. Journal of Non-Crystalline Solids. 2003;316:174–82.
[12] Freiman SW, Wiederhorn SM, Mecholsky JJ, Jr. Environmentally enhanced fracture of glass: a historical perspective. Journal of American Ceramic Society. 2009;92(7):1371–82.